The contribution of metabolic and adipose tissue inflammation to non-alcoholic fatty liver disease

Mulder, P.C.A.

Chapter 2

Surgical removal of inflamed epididymal white adipose tissue attenuates the development of non-alcoholic steatohepatitis in obesity

Petra Mulder[1,2], Martine C. Morrison[1], Peter Y. Wielinga[1], Wim van Duyvenvoorde[1], Teake Kooistra[1], Robert Kleemann[1,2]

[1] Department of Metabolic Health Research, Netherlands Organization for Applied Scientific Research (TNO), Zernikedreef 9, 2333 CK Leiden, The Netherlands
[2] Leiden University Medical Center, Department of Cardiovascular Surgery, Leiden, 2333 ZA, The Netherlands

International Journal of Obesity. 2015 Oct 26. doi:10.1038/ijo.2015.226

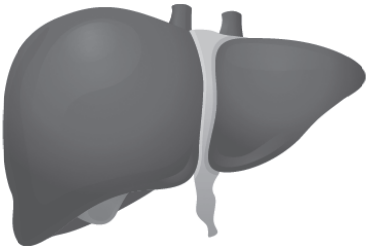

ABSTRACT

Background: Non-alcoholic fatty liver disease (NAFLD) is strongly associated with abdominal obesity. Growing evidence suggests that inflammation in specific depots of white adipose tissue (WAT) plays a key role in NAFLD progression, but experimental evidence for causal role of WAT is lacking.

Methods: A time-course study in C57BL/6J mice was performed to establish which WAT depot is most susceptible to develop inflammation during high-fat diet (HFD)-induced obesity. Crown-like structures (CLS) were quantified in epididymal (eWAT), mesenteric (mWAT) and inguinal/subcutaneous (iWAT) WAT. The contribution of inflamed WAT to NAFLD progression was investigated by surgical removal of a selected WAT depot and compared to sham surgery. Plasma markers were analyzed by ELISA (cytokines/adipokines) and lipidomics (lipids).

Results: In eWAT, CLS were formed already after 12 weeks of HFD which coincided with maximal adipocyte size and fat depot mass, and preceded establishment of non-alcoholic steatohepatitis (NASH). By contrast, the number of CLS were low in mWAT and iWAT. Removal of inflamed eWAT after 12 weeks (eWATx group), followed by another 12 weeks of HFD feeding, resulted in significantly reduced NASH in eWATx. Inflammatory cell aggregates (-40%; $p<0.05$) and inflammatory genes (e.g. TNFα, -37%; $p<0.05$) were attenuated in livers of eWATx mice, while steatosis was not affected. Concomitantly, plasma concentrations of circulating pro-inflammatory mediators, viz. leptin and specific saturated and monounsaturated fatty acids, were also reduced in the eWATx group.

Conclusion: Intervention in NAFLD progression by removal of inflamed eWAT attenuates the development of NASH and reduces plasma levels of specific inflammatory mediators. These data support the hypothesis that eWAT is causally involved in the pathogenesis of NASH.

INTRODUCTION

Non-alcoholic fatty liver disease (NAFLD) is a significant health problem and the most common form of chronic liver disease world-wide [1,2]. The prevalence of NAFLD parallels the steady increases in the rates of obesity, and consumption of saturated fat is positively associated with the risk of NAFLD [3]. Clinicopathologically, NAFLD comprises a wide spectrum of liver damage ranging from bland steatosis (NAFL) to non-alcoholic steatohepatitis (NASH), fibrosis and ultimately cirrhosis [4]. Bland steatosis is benign whereas NASH is characterized by hepatocyte injury, TNFα-mediated inflammation [4], and a high risk of liver-related morbidity and mortality [1].

The pathogenesis of NAFLD is not fully understood, and the factors that contribute to disease progression from bland steatosis to NASH remain enigmatic. Epidemiological and human observational studies do provide indications that progressive NAFLD is strongly associated with white adipose tissue (WAT) inflammation, insulin resistance, and elevated circulating levels of inflammatory mediators including certain adipokines and lipids [5-10]. Furthermore, longitudinal rodent studies demonstrated that high fat diet (HFD)-induced expression of inflammatory genes in WAT precedes the development of NASH in disease models with obesity, suggesting a potential role of inflamed WAT in NAFLD progression [11]. Also, the severity of the NAFLD pathology appears to be closely linked to WAT dysfunction, i.e. hypertrophy of adipocytes combined with macrophage infiltration, formation of crown-like structures (CLS) and enhanced expression of inflammatory genes [12]. Hence, it has been postulated that obesity-induced inflammation in WAT is critical for the development of NAFLD [13,14], but experimental evidence for an involvement of WAT is still lacking.

WAT is a complex endocrine organ that is composed of different depots among which the intra-abdominal (e.g. epididymal and mesenteric) and subcutaneous (e.g. inguinal) WAT depots [15,16]. These depots are thought to play different roles in energy storage and inflammation [13,15,16] and may thus have different contributions to the pathogenesis of NAFLD. The temporal development of inflammation (i.e. CLS formation) in WAT depots has not been systematically

investigated and it is not known whether a particular depot is more prone to become inflamed during HFD-induced obesity and associated NAFLD.

The present time-course study analyses HFD-evoked changes in epididymal (eWAT), mesenteric (mWAT) and inguinal WAT (iWAT) with specific emphasis on adipocyte hypertrophy and WAT inflammation (CLS formation). To that end, a cohort of male C57BL/6J mice was treated with HFD for a period of 24 weeks. Groups of mice were sacrificed at regular intervals, and compared to chow controls. Longitudinal histological analyses revealed that a particular depot (eWAT) is highly susceptible to develop inflammation with pronounced CLS formation after already 12 weeks. In a separate experiment, the inflamed eWAT depot of obese HFD-fed mice was surgically removed (after 12 weeks on a HFD) to examine a potential role of eWAT in the subsequent development of NASH. Our results provide evidence that inflamed eWAT plays an important role in the pathogenesis of NASH. Analysis of adipokines and circulating lipids by lipidomics supports the view that circulating inflammatory factors derived from eWAT mediate NASH development.

MATERIAL AND METHODS

Animals and housing

Animal experiments were approved by an independent Animal Care and Use Committee and were in compliance with European Community specifications for the use of laboratory animals.

Time-course cohort study

Male 9-week old wild-type C57BL/6J mice (n=84) were obtained from Charles River Laboratories (L'Arbresle Cedex, France). After an acclimatization period of 3 weeks on chow diet (R/M-H, Ssniff Spezialdieten GmbH, Soest, Germany; containing: 33 kcal% protein, 58 kcal% carbohydrate and 9 kcal% fat), mice were matched into 7 groups of n=12 mice each based on body weight. One group was sacrificed after matching to define the starting condition of the experiment (t=0). Three groups were treated with high-fat diet (HFD; D12451, Research Diets Inc., New Brunswick, USA; with 20 kcal%

protein, 35 kcal% carbohydrate and 45 kcal% lard fat) and three control groups remained on chow. Mice had ad libitum access to food and water and groups were sacrificed after 6, 12 and 24 weeks on diet respectively. Plasma samples were collected after 5h fasting at 4-week intervals. Animals were sacrificed by CO_2 asphyxiation, a serum sample was collected by heart puncture; and liver, epididymal (eWAT), mesenteric (mWAT) and inguinal (iWAT) WAT were isolated. A part of the tissues was fixed in formalin and paraffin-embedded for histological analysis, another part was snap-frozen in liquid nitrogen and stored at -80°C for real-time polymerase chain reaction (RT-PCR).

Surgical removal of epididymal adipose tissue depot (eWAT)

In a separate HFD-feeding experiment the contribution of eWAT to NASH development was analyzed. Male 9-week old wild-type C57BL/6J mice (Charles River Laboratories, L'Arbresle Cedex, France) were acclimatized for three weeks and matched in two groups (n=15/group), after 12 weeks of HFD feeding based on body weight and fasting plasma insulin concentrations. All mice were injected subcutaneously with carprofen analgesic (5 mg/kg) 30 minutes prior to surgery and anesthetized with isoflurane during surgery. In the eWATx group, both eWAT fat pads were surgically removed through a mid-ventral abdominal incision as described [17]. Testes were visualized and the attached epididymal fat pads were carefully removed and weighed, without damaging the testicular blood supply. In the sham group, a mid-ventral incision was made and the epididymal fat pads were visualized, i.e. fat pads were pulled out, but were left intact and placed back inside the peritoneal cavity. One animal from the eWATx group died during surgery and was therefore excluded from the study. Daily food intake and body weight regain were evaluated to determine recovery from surgery. After surgery, mice continued HFD feeding for another 12 weeks and were then sacrificed for histological evaluation of livers.

Histological, biochemical, lipidomic and gene expression analyses

A detailed description of biochemical, lipidomic and gene expression analyses is provided as Supplement 1. For histological analysis of livers, 5-µm-thick cross-sections were stained with Hematoxylin-Eosin (HE). NAFLD was scored blindly using a general scoring system for rodent models which is based on the human NAS grading

criteria [18]. Briefly, microvesicular steatosis and macrovesicular steatosis were separately scored and expressed as a percentage of the cross-sectional area. Hepatic inflammation was analyzed by counting the number of inflammatory foci per field at a 100x magnification (view size 3.1 mm^2) in five different fields per specimen. For WAT, paraffin-embedded cross sections (5 µm thick) were stained with Hematoxylin-Phloxine-Saffron (HPS) for quantification of adipocyte size and CLS using an Olympus BX51 microscope and Cellˆ D software (Olympus, Zoeterwoude, The Netherlands). The number of CLS was counted in 5 fields (100x magnification) per mouse and depot and data were expressed as number of CLS per 1000 adipocytes.

Statistical analysis

All data are presented as mean±SEM. Significance of differences of continuous variables between HFD fed and chow fed animals was tested using student's t-test. Changes over time between the different HFD groups (t=0, 6, 12 and 24 weeks) were statistically analyzed by One-way ANOVA and Tukey post-hoc test (normally distributed variables). Non-normally distributed variables were tested by non-parametric Kruskal-Wallis test followed by Mann-Whitney U tests. Statistical significance of differences between SHAM and eWATx was tested using unpaired one-sided t-tests. Paired two-sided t-tests were used to calculate the significance of induction of inflammatory mediators in plasma (fatty acids and adipokines) between week 12 and week 24 (i.e. before and after surgery) within each group. Results were considered statistically significant at $p<0.05$. Analyses were performed using Graphpad Prism software (version 6, Graphpad Software Inc. La Jolla, USA).

RESULTS

Time-resolved analysis of HFD-induced obesity, hyperinsulinemia and hyperglycemia in a cohort of mice

Mice had an average body weight of 26.2±1.0 g at the start of the experiment (t=0). Body weight was significantly higher in mice on a HFD compared to control mice already after 4 weeks of diet feeding and HFD-fed mice reached a final body weight

of 51.6±0.8g versus 33.3±0.7g in chow-fed control mice at 24 weeks of diet feeding (Figure 1A). HFD feeding significantly increased fasting plasma insulin (8.2±0.2 ng/mL) compared to chow (1.6±0.2 ng/mL) (Figure 1B). The HFD effect on insulin was accompanied by a significant increase in fasting plasma glucose (15.1±0.5 mM), compared to on chow (10.9±0.4 mM) (Figure 1C). Plasma triglycerides concentrations were comparable between HFD and chow treated groups and decreased slightly over time (not shown). Altogether, these data show that HFD-treated mice developed obesity, hyperinsulinemia and hyperglycemia, all of which are associated with NAFLD.

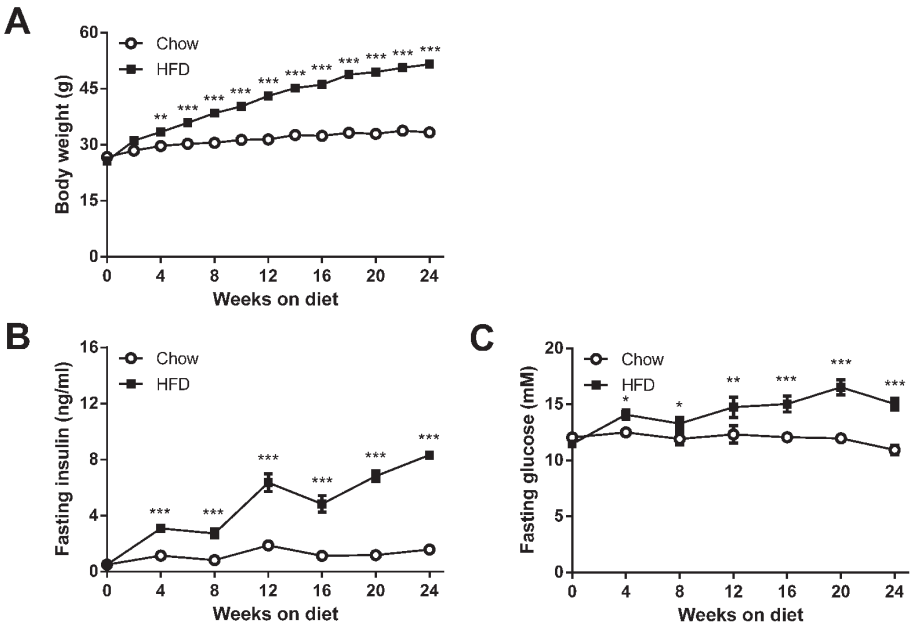

Figure 1. Time-course analysis of the effect of HFD on body weight and metabolic parameters. (A) HFD feeding increased body weight compared to chow control diet. HFD feeding gradually increased fasting plasma concentrations of (B) insulin and (C) glucose compared to chow. Data are mean±SEM (n=12/group per time point), *p<0.05,**p<0.01,***p<0.001 versus chow control.

HFD feeding induces liver steatosis by week 12 which progresses to NASH

Livers collected at t=0, 6, 12 and 24 weeks of diet feeding were analyzed for steatosis and presence of inflammatory cell aggregates to evaluate development of NASH

(representative images shown in Figure 2A). HFD feeding resulted in modest steatosis by week 12 which intensified significantly towards the end of the study, while chow-fed mice showed no steatosis and normal liver histology at all the time points (not shown). Quantification of distinct forms of steatosis, i.e. micro- and macrovesicular steatosis, demonstrated a gradual increase in HFD-induced microvesicular steatosis over time (Figure 2B). By contrast, macrovesicular steatosis (a hallmark of overt human NASH [4]) had hardly developed by week 12, but was significantly increased in week 24 (Figure 2C). HFD-induced liver steatosis can be attributed to significant increases in liver triglycerides as measured biochemically in corresponding liver homogenates (Figure 2D). Lobular inflammation was specifically induced by HFD (Figure 2E), not by chow, and showed a similar time pattern as macrovesicular steatosis. More specifically, the number of inflammatory cell aggregates (an indicator of lobular inflammation [18]) remained low until week 12 and increased significantly by week 24. HFD-induced lobular inflammation was accompanied by significantly increased TNFα and MCP-1/CCL2 gene expression in livers at t=24 weeks (Figure 2F-G).

Taken together, these data demonstrate that 12 weeks of HFD feeding resulted in bland steatosis which progressed to NASH by week 24 as demonstrated by the establishment of pronounced macrovesicular steatosis and lobular inflammation.

Epididymal WAT depot is prone to develop HFD-induced inflammation

We next examined whether the epididymal (eWAT), mesenteric (mWAT) and inguinal (iWAT) depots would differ in their susceptibility to develop inflammation during HFD-feeding and we defined the time point at which CLS formation started in the various depots. HFD-feeding led to an increase in mass of eWAT, mWAT and iWAT depots over time (Figure 3A), while the mass of the depots remained unchanged on chow (not shown). eWAT mass increased strongly at week 6 and reached a maximum already in week 12 (2.4±0.1g). By contrast, the mass of mWAT and iWAT increased continuously over time until the end of the experiment (Figure 3A). In all WAT depots, adipocytes increased in size during HFD feeding indicating that adipocyte expansion is a generic response of all WAT depots. However, the adipocytes of eWAT rapidly reached a maximal size in week 6 (Figure 3B).

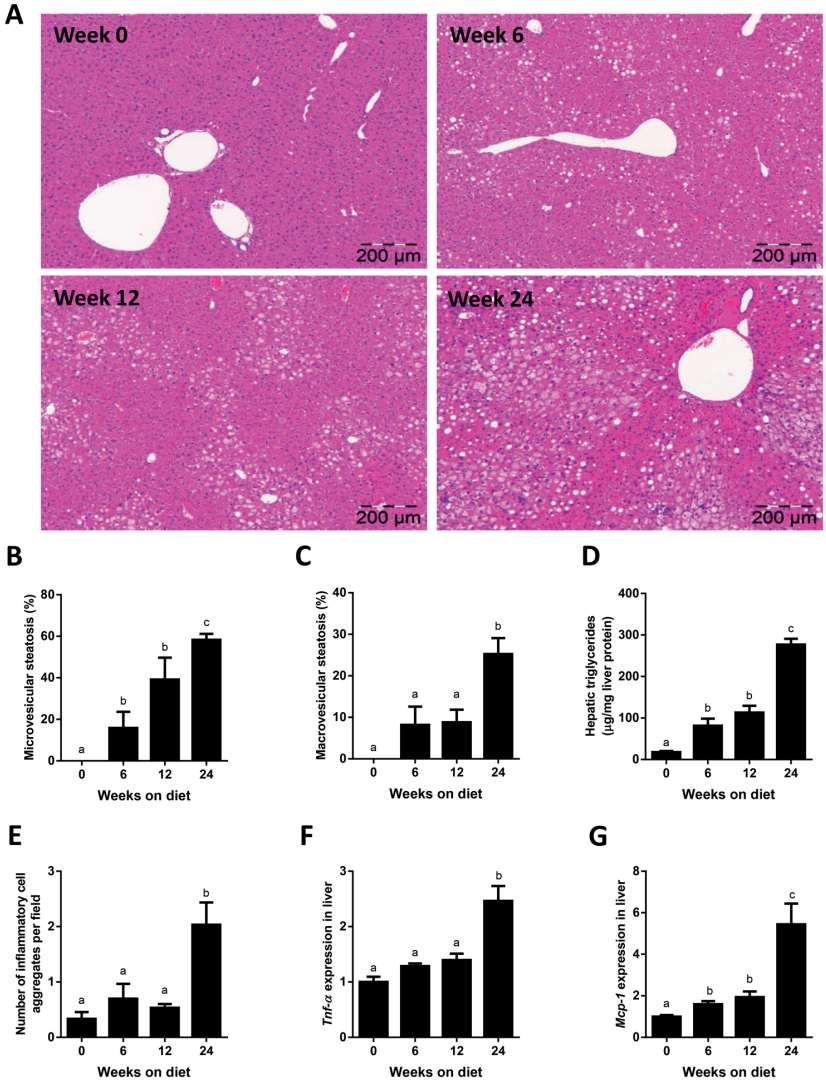

Figure 2. Time-resolved development of NAFLD induced by HFD feeding. (A) Representative photomicrographs of HE-stained liver cross-sections of mice treated with HFD for 0,6,12 or 24 weeks (magnification x100). Histological analysis of (B) microvesicular and (C) macrovesicular steatosis as percentage of the cross-sectional area (n=6-12/group per time point). (D) Biochemical quantification of hepatic triglyceride content (n=11-12/group). (E) Development of lobular inflammation in liver over time defined as the number of inflammatory cell aggregates (n=6-12/group per time point). (F) Gene expression of TNFα and (G) MCP-1 in liver over time. Data (n=8/group) are expressed as fold-change in gene expression relative to t=0. Data are mean±SEM. ^{a,b,c} Mean values with unlike letters differ significantly from each other (p<0.05).

Adipocytes in the other depots were still smaller at this time point and their size increased more slowly and gradually until the end of the study. Notably, in week 6 first CLS were observed in eWAT specifically and their numbers increased greatly in week 12 when the maximal capacity of eWAT seemed to be reached (viz. maximal mass and maximal adipocytes size) (Figure 3C). CLS formation in eWAT was more rapid and pronounced than in mWAT and iWAT (Figure 3C-D) showing that eWAT is most prone to develop HFD-induced inflammation. In mWAT, CLS numbers increased later than in eWAT (by week 24) and when maximal average adipocyte size was reached, essentially as observed in eWAT. These observations show that the expandability of a depot (and its adipocytes) is limited and that this depot-specific restriction seems critical for the development of inflammation. In all, our time-resolved histological analyses show that HFD-induced WAT inflammation starts in a specific depot (eWAT) and increases strongly when eWAT has expanded maximally (at t=12 weeks). Importantly, eWAT inflammation coincides with bland steatosis and hence precedes the development of NASH.

Surgical removal of inflamed eWAT attenuates NASH development

To examine whether eWAT is causally involved in the progression of liver steatosis to NASH, we performed a separate HFD feeding experiment in which eWAT was surgically removed in one group (eWATx) and compared to a SHAM surgery control group (SHAM). The surgery was performed after week 12 of HFD feeding, i.e. the time point at which livers in the above time-course experiment were steatotic and eWAT was inflamed.

Body weight at the time of surgery was comparable between SHAM and eWATx groups (SHAM: 42.3±1.2g, and eWATx: 42.3±0.9g; Figure 4A). On average 1.9±0.1g of eWAT was removed and this reduction in fat mass was reflected in the body weight of eWATx mice the day after surgery (SHAM: 41.6±1.7g; and eWATx: 39.5±1.2g, not shown). CLS were abundantly present in this tissue, confirming pronounced inflammation at the time of surgery (Figure 4B). Food intake was comparable between the eWATx and SHAM group throughout the study. The total body weight at the end of the experiment was 47.1±1.3 g in SHAM and 46.7±0.9 g in eWATx, and whole body fat mass determined by EchoMRI was slightly lower in

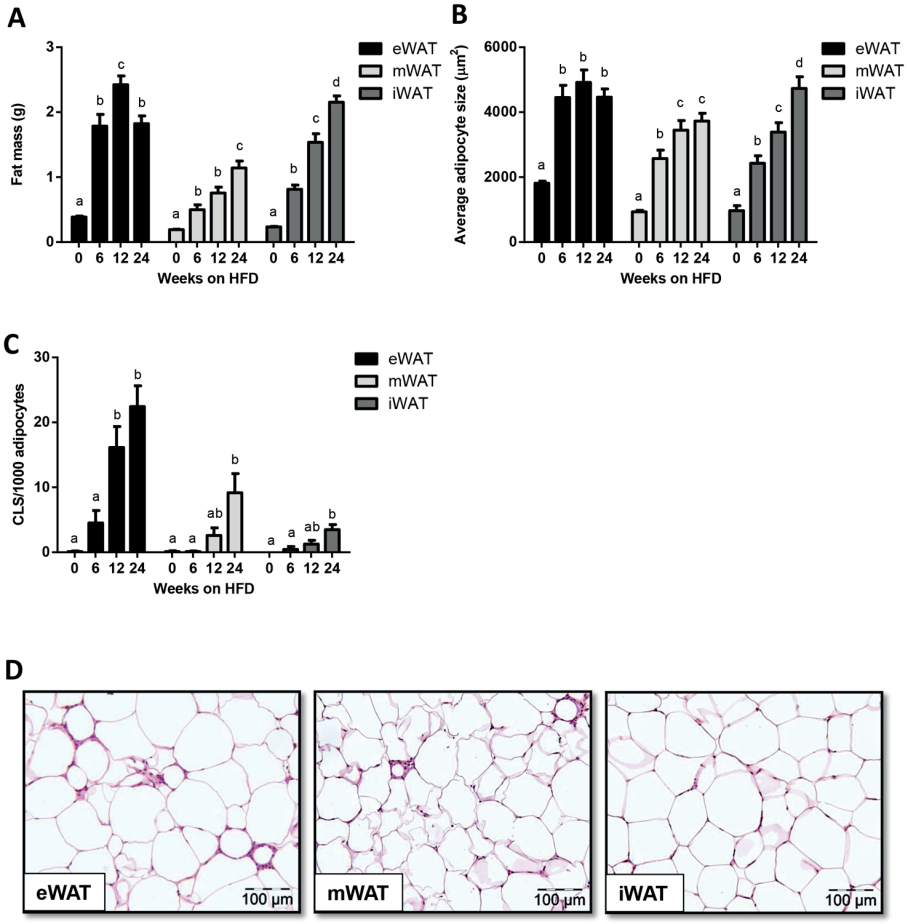

Figure 3. Effect of HFD feeding on the quantity and inflammatory state of the epididymal (eWAT), mesenteric (mWAT) and inguinal (iWAT) white adipose tissue (WAT) depots. (A) WAT mass of eWAT, mWAT and iWAT depot during HFD-feeding time-course experiment (n=12/group per time point). (B) Development of adipocyte cell size of the different WAT depots quantified by morphometric analysis of HPS-stained sections. (C) Quantitative analysis of the number of crown-like structures (CLS) in the different WAT depots over time (n=8-12/group per time point). (D) Representative images of HPS-stained cross-sections of eWAT, mWAT and iWAT after 24 weeks of HFD (magnification x200). Data are mean±SEM. ^{a,b,c,d} Mean values with unlike letters differ significantly from each other (p<0.05).

eWATx mice (not significant, Figure 4C), while lean mass was comparable between the groups (SHAM: 29.1±0.6g vs. eWATx: 29.7 ±0.4g, ns). Fasting plasma glucose concentrations increased during the experiment, essentially as observed in the time-course study, and hyperglycemia was comparable in both groups (SHAM: 14.6±0.7 mM vs. eWATx: 15.2±0.6 mM; ns). Isolation of individual fat depots after sacrifice in week 24 showed that eWAT mass was significantly reduced in eWATx (Figure 4D). The mass of mWAT, iWAT (Figure 4D) and retroperitoneal WAT (not shown) was comparable in both groups indicating that these depots did not compensate for the removed eWAT.

Histological analysis of livers revealed that eWATx mice exhibited a similar degree of micro- and macrovesicular steatosis compared with SHAM mice (Figure 5A-C). Biochemical analysis of liver triglycerides in liver homogenates showed no significant difference between the groups (SHAM: 160.8±18.9 µg/mg liver protein vs. eWATx: 170.5±16.2 µg/mg liver protein; ns). Minor liver lipids (cholesteryl esters and free cholesterol) were also comparable between the groups (data not shown). Remarkably, eWATx livers displayed a significantly reduced number of inflammatory cell aggregates indicating attenuated NASH development upon eWAT removal (Figure 5D). Reduced liver inflammation was substantiated by a significantly decreased gene expression of TNFα (Figure 5E) and MCP-1 (trend p=0.08; Figure 5F) in eWATx livers.

Collectively, these results show that surgical removal of inflamed eWAT significantly attenuates the development of NASH in absence of an effect on hyperglycemia and demonstrates a causal role of eWAT in the pathogenesis of NAFLD. We next analyzed circulating factors that could mediate this effect on liver.

Surgical removal of eWAT affects circulating levels of pro-inflammatory mediators

The effects of eWAT removal on adipokines and lipids associated with NAFLD development were assessed. In eWATx, the IL-6 serum concentrations were slightly lower (5.5±2.6 pg/ml) than in SHAM (7.0±2.5 pg/ml, not shown) but the difference was not statistical significant. The eWATx and SHAM groups also had comparable plasma concentrations of MCP-1 (86.6±11.7 pg/ml vs. 80.8±13.3 pg/ml; ns) and adiponectin (13.6±1.1 µg/ml vs. 14.3±1.2 µg/ml; ns). By contrast, plasma leptin concentrations

increased significantly in SHAM mice and this increase was not observed in eWATx mice (Figure 6A). Plasma leptin levels also correlated positively (r^2=0.7; p=0.01) with hepatic Mcp-1 expression suggesting a link to hepatic inflammation.

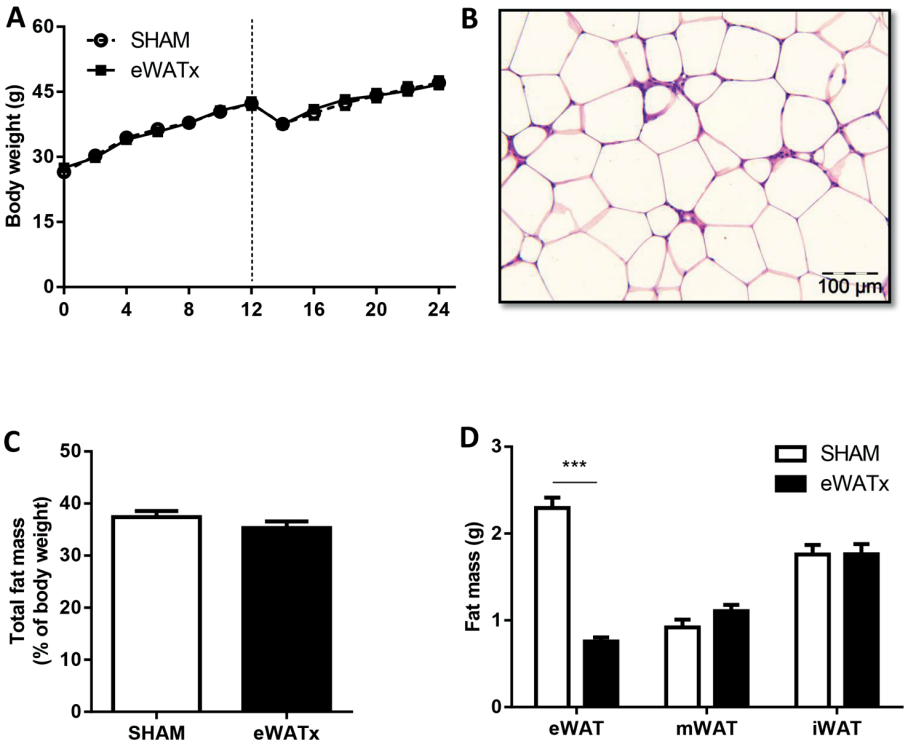

Figure 4. Effect of surgical removal of eWAT on body weight and other WAT depots. Mice were fed HFD and, on average, 1.9 gram of eWAT was carefully removed after 12 weeks of HFD. (A) Body weight development of the eWATx and SHAM group. The dashed line indicates the time point of surgery. (B) Representative image of a HPS-stained eWAT cross-section showing presence of inflammatory cells and CLS at time of removal (magnification x200). (C) Analysis of total fat mass measured by EchoMRI in week 24 of HFD. (D) Mass of eWAT, mWAT and iWAT isolated at the end of the study (24 weeks of HFD) in eWATx and SHAM group. The eWAT mass of eWATx mice was significantly lower than in SHAM. Data also show that mWAT and iWAT did not compensate for the removed eWAT. Data are mean±SEM (n=14-15/group),***p<0.001 versus SHAM.

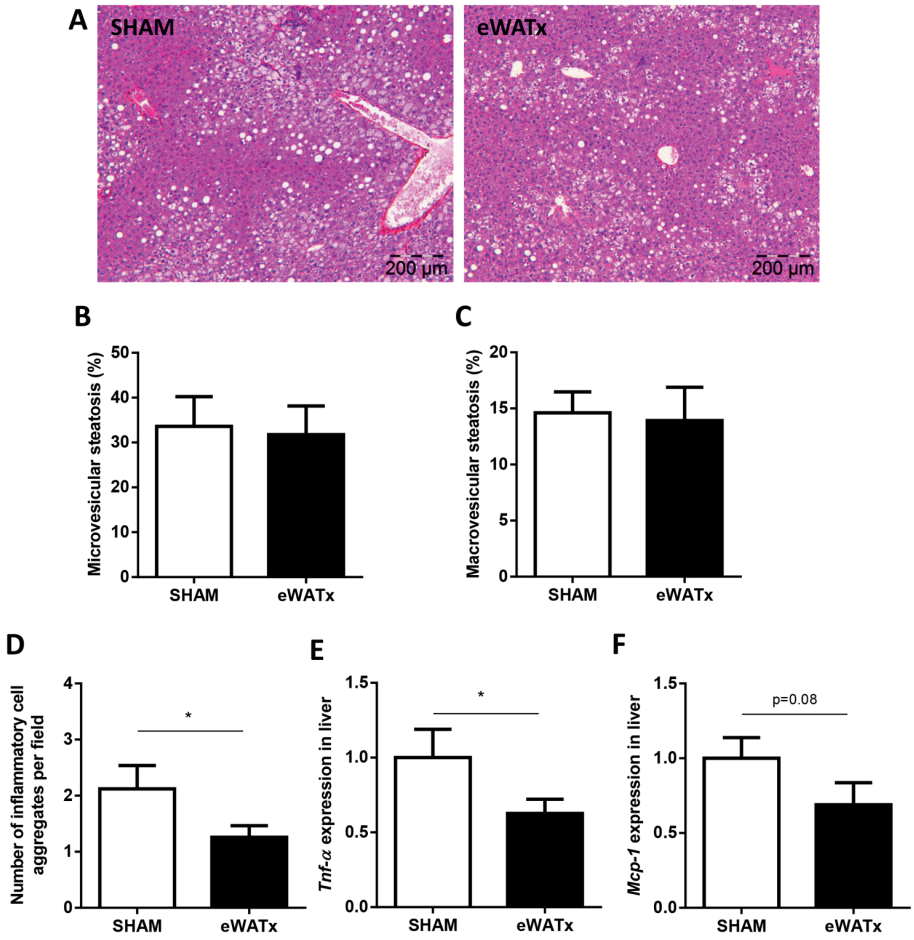

Figure 5. Effect of surgical removal of eWAT on NAFLD development. (A) Representative images of HE-stained liver sections (magnification x100). (B) Quantification of microvesicular steatosis and (C) macrovesicular steatosis as percentage of the cross-sectional liver area (n=14-15/group). (D) Number of inflammatory cell aggregates in livers of eWATx and SHAM mice. Liver gene expression of (E) TNFα and (F) MCP-1 in eWATx and SHAM. Real-time PCR data are expressed as fold-change in gene expression relative to SHAM (n=8/group). Data are mean±SEM,*p<0.05.

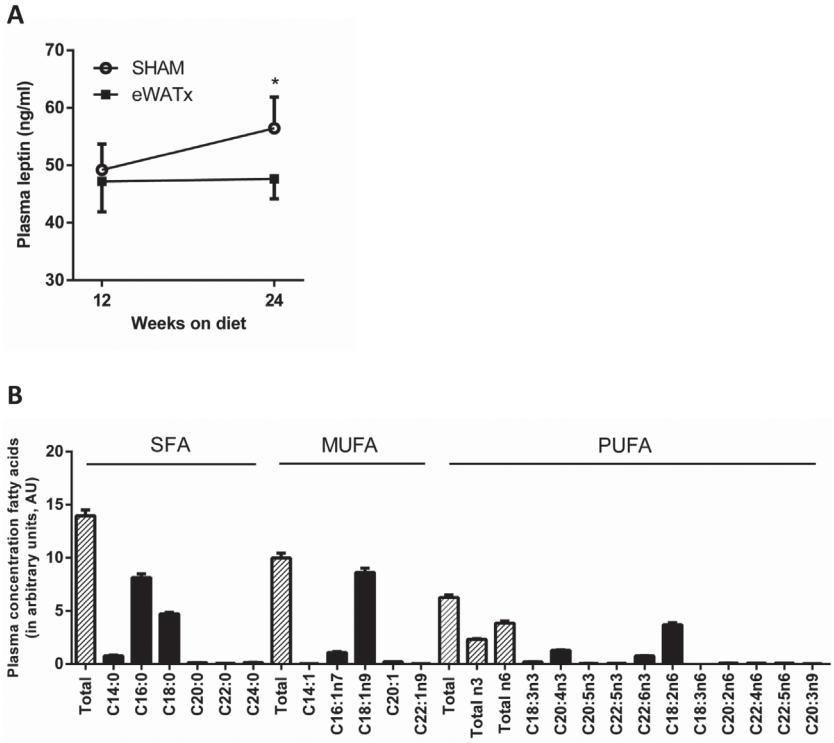

Figure 6. Effect of surgical removal of eWAT on circulating inflammatory mediators and lipids. (A) Plasma concentrations of leptin prior to surgery at 12 weeks of HFD, and at the end of the experiment (24 weeks) in eWATx and SHAM group. Data are mean±SEM,*p<0.05 according to paired Student's t-test. (B) Profiling of plasma lipids after 12 weeks of HFD by lipidomic analysis. Fasting plasma was collected before surgery. The levels of saturated free fatty acids (SFA), monounsaturated fatty acids (MUFA) and polyunsaturated fatty acids (PUFA) are shown and the most abundant lipid species of each category are indicated. Data are mean±SEM and expressed as arbitrary units (AU) relative to internal standard.

We next profiled the circulating (pro-inflammatory) lipids using lipidomics to define the most abundant lipid species in plasma (Figure 6B), and subsequently analyzed whether eWATx removal affected these lipids (Table 1). Saturated fatty acids (SFA) were the most abundant lipid species after 12 weeks of HFD feeding (prior to surgery), followed by monounsaturated fatty acids (MUFA), and n-6 and n-3 polyunsaturated fatty acids (PUFA) (Figure 6B). Within the SFA, C16:0 (palmitic acid), C18:0 (stearic acid) and C14:0 (myristic acid) were most abundant. Within the

class of MUFA C18:1n9 (oleic acid) and C16:1n7 (palmitoleic acid) were circulating at high levels, and within the PUFA, C20:4n3 (eicosatetraenoic acid) and C18:2n6 (linoleic acid) were most abundant.

Table 1 shows that the level of total SFA, and palmitic acid in particular (+1.4; $p<0.05$), increase in SHAM while such an increase was not observed in eWATx. Myristic acid and several of the less abundant SFA (C20:0, C22:0, C24:0) decreased significantly after eWAT removal. Furthermore, total MUFA increased strongly over time in SHAM (+3.7; $p<0.05$), mainly due to significant rises in palmitoleic, oleic and eicosenoic acids. By contrast, there was no significant change over time in any of the MUFA in the eWATx group. Total PUFA levels increased in both, SHAM (+2.0) and eWATx (+1.5). The observed changes in SFA and MUFA support the notion that removal of eWAT prevents the development of a pro-inflammatory state.

DISCUSSION

NAFLD is strongly associated with obesity but the pathogenesis of the disease, and in particular the role of WAT, is poorly understood. It has been proposed that inflammation in WAT may play a critical role in obesity-induced NAFLD development [4,13,19,20], but evidence for causality is lacking. This study shows that HFD-induced inflammation in eWAT develops more rapidly than in mWAT or iWAT, and that this inflammation precedes overt NASH. Notably, pronounced CLS formation was observed in eWAT once the adipocytes of this tissue did not further increase in size and the depot had reached a maximal mass (week 12 of HFD feeding). A subsequent experiment showed that removal of the inflamed eWAT depot at week 12 attenuates liver inflammation and reduces the development of NASH. Removal of eWAT affected the circulating levels of specific pro-inflammatory mediators among which leptin and specific lipids (e.g. palmitic acid), providing a rationale for the observed hepatoprotective effect.

The time-course analysis of HFD-induced NAFLD shows that a particular intra-abdominal depot in mice, eWAT, is prone to develop tissue inflammation characterized by presence of macrophages and CLS. Consistent with this finding,

Table 1. Change in plasma fatty acid levels in SHAM and eWATx

Fatty acids	SHAM Δ change	eWATx Δ change
Saturated fatty acid (SFA)	**1.3 ± 0.8**	**-0.3 ± 1.0**
Myristic acid (C14:0)	0.02 ± 0.1	-0.3 ± 0.2
Palmitic acid (C16:0)	1.4 ± 0.5*	-0.1 ± 0.6
Stearic acid (C18:0)	-0.03 ± 0.3	0.4 ± 0.2
Arachidic acid (C20:0)	-0.01 ± 0.0	-0.05 ± 0.0*
Behenic acid (C22:0)	-0.01 ± 0.0	-0.04 ± 0.0*
Lignoceric acid (C24:0)	-0.02 ± 0.0	-0.1 ± 0.1*
Monounsaturated acid fatty acid (MUFA)	**3.7 ± 0.9*#**	**0.8 ± 0.8**
Myristoleic acid (C14:1)	0.0 ± 0.0	0.0 ± 0.0
Palmitoleic acid (C16:1n7)	0.5 ± 0.2*	0.2 ± 0.1
Oleic acid (C18:1n9)	3.1 ± 0.8*#	0.6 ± 0.7
Eicosenoic acid (C20:1)	0.1 ± 0.0*	0.03 ± 0.0
Erucic acid (C22:1n9)	0.004 ± 0.0	-0.003 ± 0.0
Polyunsaturated fatty acid (PUFA)	**2.0 ± 0.6***	**1.5 ± 0.4***
Total n6-fatty acids	1.7 ± 0.5*	1.0 ± 0.3*
Total n3-fatty acids	0.3 ± 0.1*	0.5 ± 0.1*
Linoleic acid (C18:2n6)	1.7 ± 0.5*	1.0 ± 0.3*
γ-linolenic acid (C18:3n6)	0.0 ± 0.0	0.0 ± 0.0
Eicosadienoic acid (C20:2n6)	0.03 ± 0.0*	0.02 ± 0.0*
Adrenic acid (C22:4n6)	0.02 ± 0.0*	0.03 ± 0.0*
Docosapentaenoic acid (C22:5n6)	0.02 ± 0.0*	0.01 ± 0.0
α-linolenic acid (C18:3n3)	0.1 ± 0.0	0.2 ± 0.0
Eicosatetraenoic acid (C20:4n3)	0.1 ± 0.1	0.3 ± 0.1*
Eicosapentaenoic acid (C20:5n3)	0.01 ± 0.0	0.01 ± 0.0*
Docosapentaenoic acid (C22:5n3)	0.01 ± 0.0*	0.02 ± 0.0*
Docosahexaenoic acid (C22:6n3)	0.1 ± 0.0*	0.1 ± 0.0*
Mead acid (C20:3n9)	0.01 ± 0.0*	0.01 ± 0.0*

Delta (Δ) change in plasma lipids between week 12 and 24, i.e. before and after surgery. Data are in arbitrary units (mean±SEM). *$p \leq 0.05$ indicates significant changes over time within a group. #$p < 0.05$ indicates significant difference between SHAM (n=11) and eWATx (n=12).

other groups have reported that eWAT of obese HFD-treated mice exhibits a higher number of CLS than mesenteric and subcutaneous (inguinal) WAT depots [21,22]. Differences in macrophage content appear to exist already in lean C57BL6 mice: Altinas et al. [21] showed that the subcutaneous depot differs from the intra-abdominal depots with respect to immune cell composition and density. For instance, the density of solitary adipose tissue macrophages (ATM) in subcutaneous WAT is much lower than in intra-abdominal depots such as eWAT [21]. Hence,

the relatively high number of solitary ATM in eWAT may predispose this depot to develop CLS more rapidly in response to HFD than other depots analyzed in this study. In obese subjects, CLS are also more prevalent in abdominal (omental) WAT than in subcutaneous WAT [6,23] suggesting that, in humans, intra-abdominal depots are also more prone to become inflamed than subcutaneous depots, and that our observations are not restricted to mice.

We found that the number of CLS in eWAT increased strongly once this depot had reached a maximal mass and concomitantly no further increase in adipocyte size was observed. In line with this, other groups reported that the weight of eWAT does typically not exceed about 2.5 grams [12,22,24,25]. This limitation in eWAT mass has been observed with different diets and in different strains of mice pointing to a generic threshold of eWAT independent of the experimental conditions employed. Consistent with this, Virtue and Vidal-Puig [26] proposed that organisms possess a maximum capacity for adipose expansion, and failure in the capacity for adipose tissue expansion, rather than obesity per se may underlie the development of inflammation. Indeed, also in the case of mWAT, CLS numbers increased at week 24, i.e. after the average adipocyte size had reached a maximum. Little is known about the mediators that control WAT expansion during diet-induced obesity. It is possible that localized cytokine production limits further WAT expansion: Salles et al. [27] showed that TNFα knockout mice have two-fold more eWAT mass than wild-type mice during HFD feeding. In support of this notion, increased TNFα gene expression in eWAT was observed after attainment of maximal adipocyte size in an experiment conducted under conditions comparable to those applied herein [22]. Together, our time-resolved analysis of the inflammatory component in diet-induced obesity shows that WAT inflammation develops sequentially across depots.

C57BL/6 mice constitute a frequently used model to study diet-induced obesity and associated comorbidities. For the interpretation of these studies, it is important to recognize that development of inflammation upon HFD-feeding is a very complex and dynamic process involving multiple tissues, including WAT and liver [11,15]. As demonstrated herein, the different WAT depots become inflamed at specific time points during HFD feeding, rather than simultaneously. Because animal studies often analyze a single WAT depot (frequently the eWAT) at one

particular time point during HFD feeding, conclusions about the condition 'adipose tissue in general' or the inflammatory state in other depots should be made with caution. Our results support a more comprehensive analysis of WAT (with precise specification of the intra-abdominal depots analyzed), and advocates the study of the cross-talk between organs in NAFLD. For instance, between 12 and 24 weeks of HFD, i.e. the period in which eWAT was inflamed and did not further expand, we observed a pronounced increase of triglyceride concentrations in the liver. This supports the concept that, once the expansion limit of a particular WAT depot has been reached, adipose tissue ceases to store energy efficiently and lipids begin to accumulate as ectopic fat in other tissues [26].

In patients, the accumulation of intra-abdominal WAT is strongly associated with progressive NASH [5]. Hepatic inflammation and fibrosis augmented incrementally with increases in intra-abdominal fat mass. Importantly, intra-abdominal fat of patients was directly associated with liver inflammation and fibrosis independent of insulin resistance and hepatic steatosis [5,7]. Consistent with this, removal of eWAT in the present study attenuated NASH development without an effect on hyperinsulinemia, hyperglycemia and liver steatosis. A possible explanation for the strong association between abdominal WAT mass and NASH severity in the liver may lie in the anatomical distance between both tissues. Inflammatory mediators from the intra-abdominal depots can reach the liver relatively easily (venous drainage via the portal vein) [28]. By contrast, associations between systemically drained adipose tissue depots (e.g. the deep layer of subcutaneous WAT in the abdominal area) and NASH are rare [29] suggesting that these depots only play a minor role in the pathogenesis of NASH.

While the above studies mainly focused on the quantity of adipose tissue, increasing evidence also points to a role of its inflammatory state. Livers of obese subjects with inflamed intra-abdominal (omental) WAT contain more fibro-inflammatory lesions than livers of equally obese subjects without WAT inflammation [6,7]. This observation suggests that inflammation in a specific WAT depot contributes to the inflammatory component in human NASH. The present study supports this view, because surgical removal of inflamed eWAT reduces liver inflammation (about 40% less inflammatory aggregates). Of note, intra-abdominal

eWAT in mice has no human equivalent and our findings should not be generalized with respect to the role of other WAT depots. Because of the close relationship between visceral obesity and NASH development in patients [5], it is possible that inflamed visceral WAT depots, such as mesenteric WAT, may contribute to NASH in a similar way as eWAT. For instance, mesenteric WAT develops similar features of inflammation as observed in eWAT, including formation of CLS during WAT expansion and expression of pro-inflammatory mediators (e.g. cytokines, adipokines, fatty acids), in both, mice [30,31] and humans [32,33]. Furthermore, pro-inflammatory mediators that are released by mesenteric WAT can reach the liver not only via systemic drainage (like eWAT) but also via the portal vein, which constitutes a more direct connection to the liver [28]. However, additional studies are needed to investigate the contribution of inflamed mesenteric WAT to NASH development.

Specific circulating factors have been proposed as inducers of liver inflammation in NASH [19,20]. Among these mediators are cytokines/adipokines (including IL-6, TNFα, leptin, adiponectin) and specific lipids with reported activities on liver cells [4,13,14,20]. Of the adipokines measured in the present study, only plasma leptin differed between the eWATx and the SHAM group. Several studies have shown that leptin exerts pro-inflammatory and pro-fibrogenic effects on liver cells [34,35]. For instance, leptin stimulates hepatic stellate cells to express the pro-inflammatory cytokine MCP-1 [35], a chemotactic factor and critical mediator of lobular inflammation [36]. In line with this, we observed that plasma leptin concentrations correlated with MCP-1 gene expression in the liver. Besides cytokines/adipokines, certain lipid mediators (e.g. SFA with TLR4 binding properties) have also been implicated in the pathogenesis of NASH. For example, *in vitro* studies have shown that SFA, and in particular palmitic acid, can trigger inflammation via the NFκB pathway and thereby induce TNFα production [37]. In SHAM mice, palmitic acid levels increased significantly between 12 and 24 weeks of HFD feeding, i.e. during the progression from NAFL to NASH. This increase was not observed in eWATx mice and in line with this, hepatic TNFα expression was lower than in SHAM. A total plasma lipid analysis in humans showed that obese subjects with NAFL and NASH have significantly elevated MUFA levels when compared with lean controls [38].

Among these MUFA were palmitoleic acid and oleic acid, which also increased after surgery in SHAM while they did not change significantly in eWATx. The observed increases in MUFA (both in humans and mice) may be an adaptive response to protect the liver from the lipotoxic effects of SFA (i.e. palmitic acid). As MUFAs themselves can suppress liver inflammation in mice [39], it is thus likely that increased levels of palmitic acid in SHAM mice are critical for the development of liver inflammation.

Collectively, this study demonstrates that obesity-induced inflammation develops progressively across various WAT depots, starting in eWAT. Surgical removal of inflamed eWAT shows that this depot participates in the development of NASH. Hence, interventions that target WAT may have significant therapeutic benefit for the treatment of NASH in the context of obesity.

ACKNOWLEDGEMENTS

The authors thank Joline Attema, Erik Offerman, Karin Toet and Simone van der Drift-Droog for their excellent technical assistance. This work was funded by TNO research programs ‘Predictive Health Technologies’ and ‘Enabling Technology Systems Biology’.

REFERENCES

1. Loomba R, Sanyal AJ. The global NAFLD epidemic. Nature reviews Gastroenterology & hepatology 2013;10:686-690.
2. de Alwis NM, Day CP. Non-alcoholic fatty liver disease: the mist gradually clears. Journal of hepatology 2008;48 Suppl 1:S104-112.
3. Musso G, Gambino R, De Michieli F, Cassader M, Rizzetto M, Durazzo M, et al. Dietary habits and their relations to insulin resistance and postprandial lipemia in nonalcoholic steatohepatitis. Hepatology 2003;37:909-916.
4. Tiniakos DG, Vos MB, Brunt EM. Nonalcoholic fatty liver disease: pathology and pathogenesis. Annual review of pathology 2010;5:145-171.
5. van der Poorten D, Milner KL, Hui J, Hodge A, Trenell MI, Kench JG, et al. Visceral fat: a key mediator of steatohepatitis in metabolic liver disease. Hepatology 2008;48:449-457.
6. Cancello R, Tordjman J, Poitou C, Guilhem G, Bouillot JL, Hugol D, et al. Increased infiltration of macrophages in omental adipose tissue is associated with marked hepatic lesions in morbid human obesity. Diabetes 2006;55:1554-1561.
7. Tordjman J, Poitou C, Hugol D, Bouillot JL, Basdevant A, Bedossa P, et al. Association between omental adipose tissue macrophages and liver histopathology in morbid obesity: influence of glycemic status. Journal of hepatology 2009;51:354-362.
8. Krawczyk K, Szczesniak P, Kumor A, Jasinska A, Omulecka A, Pietruczuk M, et al. Adipohormones as prognostric markers in patients with nonalcoholic steatohepatitis (NASH). Journal of physiology and pharmacology : an official journal of the Polish Physiological Society 2009;60 Suppl 3:71-75.
9. Lemoine M, Ratziu V, Kim M, Maachi M, Wendum D, Paye F, et al. Serum adipokine levels predictive of liver injury in non-alcoholic fatty liver disease. Liver international : official journal of the International Association for the Study of the Liver 2009;29:1431-1438.
10. Nehra V, Angulo P, Buchman AL, Lindor KD. Nutritional and metabolic considerations in the etiology of nonalcoholic steatohepatitis. Dig Dis Sci 2001;46:2347-2352.
11. Liang W, Tonini G, Mulder P, Kelder T, van Erk M, van den Hoek AM, et al. Coordinated and interactive expression of genes of lipid metabolism and inflammation in adipose tissue and liver during metabolic overload. PloS one 2013;8:e75290.
12. Duval C, Thissen U, Keshtkar S, Accart B, Stienstra R, Boekschoten MV, et al. Adipose tissue dysfunction signals progression of hepatic steatosis towards nonalcoholic steatohepatitis in C57BL/6 mice. Diabetes 2010;59:3181-3191.
13. Tordjman J, Guerre-Millo M, Clement K. Adipose tissue inflammation and liver pathology in human obesity. Diabetes & metabolism 2008;34:658-663.
14. Suganami T, Tanaka M, Ogawa Y. Adipose tissue inflammation and ectopic lipid accumulation. Endocr J 2012;59:849-857.
15. Caesar R, Manieri M, Kelder T, Boekschoten M, Evelo C, Muller M, et al. A combined transcriptomics and lipidomics analysis of subcutaneous, epididymal and mesenteric adipose tissue reveals marked functional differences. PloS one 2010;5:e11525.
16. Cinti S. The adipose organ: morphological perspectives of adipose tissues. The Proceedings of the Nutrition Society 2001;60:319-328.
17. Harris RB, Hausman DB, Bartness TJ. Compensation for partial lipectomy in mice with genetic alterations of leptin and its receptor subtypes. Am J Physiol Regul Integr Comp Physiol 2002;283:R1094-1103.
18. Liang W, Menke AL, Driessen A, Koek GH, Lindeman JH, Stoop R, et al. Establishment of a general NAFLD scoring system for rodent models and comparison to human liver pathology. PloS one 2014;9:e115922.

19. Tilg H, Moschen AR. Evolution of inflammation in nonalcoholic fatty liver disease: the multiple parallel hits hypothesis. Hepatology 2010;52:1836-1846.
20. Mirza MS. Obesity, Visceral Fat, and NAFLD: Querying the Role of Adipokines in the Progression of Nonalcoholic Fatty Liver Disease. ISRN gastroenterology 2011;2011:592404.
21. Altintas MM, Azad A, Nayer B, Contreras G, Zaias J, Faul C, et al. Mast cells, macrophages, and crown-like structures distinguish subcutaneous from visceral fat in mice. Journal of lipid research 2011;52:480-488.
22. Strissel KJ, Stancheva Z, Miyoshi H, Perfield JW, 2nd, DeFuria J, Jick Z, et al. Adipocyte death, adipose tissue remodeling, and obesity complications. Diabetes 2007;56:2910-2918.
23. Harman-Boehm I, Bluher M, Redel H, Sion-Vardy N, Ovadia S, Avinoach E, et al. Macrophage infiltration into omental versus subcutaneous fat across different populations: effect of regional adiposity and the comorbidities of obesity. The Journal of clinical endocrinology and metabolism 2007;92:2240-2247.
24. Lagathu C, Christodoulides C, Tan CY, Virtue S, Laudes M, Campbell M, et al. Secreted frizzled-related protein 1 regulates adipose tissue expansion and is dysregulated in severe obesity. International journal of obesity 2010;34:1695-1705.
25. Larter CZ, Yeh MM, Van Rooyen DM, Teoh NC, Brooling J, Hou JY, et al. Roles of adipose restriction and metabolic factors in progression of steatosis to steatohepatitis in obese, diabetic mice. Journal of gastroenterology and hepatology 2009;24:1658-1668.
26. Virtue S, Vidal-Puig A. Adipose tissue expandability, lipotoxicity and the Metabolic Syndrome--an allostatic perspective. Biochim Biophys Acta 2010;1801:338-349.
27. Salles J, Tardif N, Landrier JF, Mothe-Satney I, Guillet C, Boue-Vaysse C, et al. TNFalpha gene knockout differentially affects lipid deposition in liver and skeletal muscle of high-fat-diet mice. The Journal of nutritional biochemistry 2012;23:1685-1693.
28. Item F, Konrad D. Visceral fat and metabolic inflammation: the portal theory revisited. Obesity reviews : an official journal of the International Association for the Study of Obesity 2012;13 Suppl 2:30-39.
29. Tordjman J, Divoux A, Prifti E, Poitou C, Pelloux V, Hugol D, et al. Structural and inflammatory heterogeneity in subcutaneous adipose tissue: relation with liver histopathology in morbid obesity. Journal of hepatology 2012;56:1152-1158.
30. Kwon EY, Shin SK, Cho YY, Jung UJ, Kim E, Park T, et al. Time-course microarrays reveal early activation of the immune transcriptome and adipokine dysregulation leads to fibrosis in visceral adipose depots during diet-induced obesity. BMC Genomics 2012;13:450.
31. Murano I, Barbatelli G, Parisani V, Latini C, Muzzonigro G, Castellucci M, et al. Dead adipocytes, detected as crown-like structures, are prevalent in visceral fat depots of genetically obese mice. Journal of lipid research 2008;49:1562-1568.
32. Fain JN, Madan AK, Hiler ML, Cheema P, Bahouth SW. Comparison of the release of adipokines by adipose tissue, adipose tissue matrix, and adipocytes from visceral and subcutaneous abdominal adipose tissues of obese humans. Endocrinology 2004;145:2273-2282.
33. Bigornia SJ, Farb MG, Mott MM, Hess DT, Carmine B, Fiscale A, et al. Relation of depot-specific adipose inflammation to insulin resistance in human obesity. Nutrition & diabetes 2012;2:e30.
34. Ikejima K, Honda H, Yoshikawa M, Hirose M, Kitamura T, Takei Y, et al. Leptin augments inflammatory and profibrogenic responses in the murine liver induced by hepatotoxic chemicals. Hepatology 2001;34:288-297.

35. Aleffi S, Petrai I, Bertolani C, Parola M, Colombatto S, Novo E, et al. Upregulation of proinflammatory and proangiogenic cytokines by leptin in human hepatic stellate cells. Hepatology 2005;42:1339-1348.
36. Marra F, Tacke F. Roles for chemokines in liver disease. Gastroenterology 2014;147:577-594 e571.
37. Shi H, Kokoeva MV, Inouye K, Tzameli I, Yin H, Flier JS. TLR4 links innate immunity and fatty acid-induced insulin resistance. The Journal of clinical investigation 2006;116:3015-3025.
38. Puri P, Wiest MM, Cheung O, Mirshahi F, Sargeant C, Min HK, et al. The plasma lipidomic signature of nonalcoholic steatohepatitis. Hepatology 2009;50:1827-1838.
39. Guo X, Li H, Xu H, Halim V, Zhang W, Wang H, et al. Palmitoleate induces hepatic steatosis but suppresses liver inflammatory response in mice. PloS one 2012;7:e39286.

SUPPLEMENTAL DATA

Supplement 1. Detailed material and methods

Biochemical analyses of circulating factors

Plasma was obtained via tail vein bleeding after a 5-hour fast at multiple time points throughout the study. Plasma glucose was quantified by hexokinase method (Instruchemie, Delfzijl, The Netherlands) and plasma insulin was determined by ELISA (Ultrasensitive mouse insulin ELISA, Mercodia, Uppsala, Sweden). Leptin and adiponectin plasma levels and Mcp-1 serum levels were determined by ELISA (all R&D Systems Ltd, Abington, UK). Serum concentrations of IL-6 and TNFα were quantified by quantikine ELISA assay (R&D Systems Ltd, Abington, UK). TNFα levels were below the detection limit, therefore excluded from the analysis. Lipidomic analysis was performed in plasma samples collected after 5 hours of fasting and according an well-established method for polar lipids, and without hydrolysis of lipids as reported earlier [1]. Reported lipids were identified and quantified using respective specific standards, except for C14:1 (reported as myristoleic acid) and C20:1 (reported as eicosenoic acid). Lipids are expressed as arbitrary units (AU) relative to internal standard.

Analysis of intrahepatic triglycerides

For determination of liver triglycerides, lipids were extracted from liver homogenates using the Bligh and Dyer method [2]. High performance thin-layer chromatography (HPTLC) was then used to separate the extracted lipids with a silica-gel-60 pre-coated plate. Density areas were measured with a Hewlett Packard Scanjet 4500c and lipid concentrations were calculated by Tina software (version-2.09).

Body composition

Total body fat and lean mass in SHAM and eWATx mice was determined using a NMR Echo MRI whole body composition analyzer (EchoMRI LLC, Houston, TX, USA) at week 24 of HFD feeding. Total body fat mass was expressed as percentage of total body weight.

Real Time Poly chain reaction (RT-PCR) gene expression analysis

Total RNA was extracted with RNA Bee Total RNA Isolation Kit (Bio-Connect, Huissen, the Netherlands). RNA concentration was determined using Nanodrop 1000 (Isogen Life Science, De Meern, the Netherlands) and RNA quality was measured using 2100 Bioanalyzer (Agilent Technologies, Amstelveen, the Netherlands). One microgram of total RNA was used to generate cDNA for RT-PCR (High-capacity RNA-to-cDNA kit; 4387406, Life Technologies, Bleiswijk, the Netherlands). RT-PCR was performed in duplicate on a Fast-7500 using TaqMan gene expression assays (Life Technologies) and specific probe for TNFα (*Tnf,* Mm00443258_m1) and MCP-1(*Ccl2,* Mm00441242_m1). Glyceraldehyde 3-phosphate dehydrogenase (*Gapdh*; 4308313) and hypoxanthine-guanine phosphoribosyltransferase (*Hprt*; Mm00446968_m1) were used as housekeeping genes. Changes in gene expression were calculated using the comparative Ct (ΔΔCt) method and expressed as fold-change relative to mean expression of control.

References Supplement 1

1. Wopereis S, Radonjic M, Rubingh C, Erk M, Smilde A, Duyvenvoorde W, et al. Identification of prognostic and diagnostic biomarkers of glucose intolerance in ApoE3Leiden mice. Physiol Genomics 2012;44:293-304.
2. Bligh EG, Dyer WJ. A rapid method of total lipid extraction and purification. Canadian journal of biochemistry and physiology 1959;37:911-917.